High Velocity Compressible Viscous Flow

HENRY G. SCHWARTZBERG and MICHAEL GUREVICH

New York University, New York, New York

Pressure drops were measured for the high velocity isothermal viscous flow of steam in circular tubes. For the velocities tested, up to 0.48 times the isothermal sonic velocity, these flows obeyed the following equation with an average deviation of 2.4%.

$$P_1^2 - P_2^2 = \frac{8\mu RTG}{DM}\left[\frac{8L}{D} + \frac{N_{Re}}{3}\ln\left(\frac{P_1}{P_2}\right)\right]$$

This equation differs from the Poiseuille-Meyer equation commonly used to correlate isothermal viscous flow in that it includes the term $(N_{Re}/3)\ln(P_1/P_2)$ which accounts for the change in momentum caused by expansion. In deriving this equation, the mean velocity, mean squared velocity, and wall shear stress were obtained from the parabolic velocity distribution for normal viscous flow. The velocity profile should flatten as the isothermal Mach number increases, and it is therefore anticipated that somewhere above the range tested the equation will no longer prove applicable. Variants of the equation, which take into account the flattening of the velocity profile in the range tested, did not fit the experimental data quite as well.

BACKGROUND

Isothermal viscous flow of gas and vapor is of considerable importance in vacuum processing. When slip flow and free molecular flow do not occur, the Poiseuille-Meyer equation is usually used to predict pressure drop for such flow. In deriving the Poiseuille-Meyer equation, momentum changes due to expansion are assumed negligible. For flows caused by condensation, velocities are often so large that momentum changes can't be neglected. Such flows are encountered in vacuum freeze drying, for example, and the corresponding flow rate and pressure drop limitations are major considerations in the design of high productivity freeze drying equipment. Pressure drop correlations for such flows are discussed herein.

Kuo (3), in a theoretical analysis of isothermal viscous compressible flow in circular tubes, developed corrections for the velocity profile and pressure drop in terms of series in ascending even powers of $\overline{Mai}$, the average isothermal Mach number. The limits of convergence for these series are not known. Kuo states that they are probably applicable only at low Mach numbers. His velocity profile equation, shown below including only the relatively simple first-order correction, indicates a flattening of the profile at high velocities:

$$\frac{U}{\overline{U}} = 2\left[1 - \left(\frac{r}{A}\right)^2\right] - \frac{4}{9}\overline{Mai}^2\left[2 - 9\left(\frac{r}{A}\right)^2 + 9\left(\frac{r}{A}\right)^4 - 2\left(\frac{r}{A}\right)^6\right] \quad (1)$$

Shang and Bloom (6), in a numerical analysis of compressible flow in two-dimensional adiabatic channels, also predicted a flattening of the velocity profile at high velocities.

The Poiseuille-Meyer equation, which is valid at low velocities, is Poiseuille's equation evaluated at a density corresponding to the arithmetic mean pressure. At low velocity, Kuo's pressure drop equation reduces to Poiseuille's equation at the exit pressure density and is therefore suspect.

MACROSCOPIC MOMENTUM BALANCE

A simple correction for the Poiseuille-Meyer equation can be obtained from the macroscopic momentum balance for a stream with a parabolic velocity profile. Because of the anticipated changes in velocity profile, this probably is an oversimplification, but it may provide a basis for higher-order corrections. For gas flowing in a circular tube, with gravitational forces neglected, such a balance (*1*) is

$$\overline{\tau_w}\pi DL = -\Delta\left[\frac{\overline{U^2}}{\overline{U}}\left(\frac{G\pi D^2}{4}\right) + \frac{\pi D^2 P}{4}\right] \quad (2)$$

For a parabolic velocity, $\overline{U^2}/\overline{U} = 4\overline{U}/3$, and for a gas, $\overline{U} = GRT/PM$. Making these substitutions, assuming isothermal conditions, and letting the difference Δ become differentially small, we obtain

$$4\tau_w dL = D\left[\frac{4}{3}\cdot\frac{G^2RT}{M}\frac{dP}{P^2} - dP\right] \quad (3)$$

where the local value τ_w can be used instead of $\overline{\tau_w}$. For a parabolic profile, $\tau_w = 8\mu\overline{U}/D = 8\mu GRT/DPM$. Substituting for τ_w, integrating, and rearranging, we obtain:

$$P_1^2 - P_2^2 = \frac{8\mu RTG}{DM}\left[\frac{8L}{D} + \frac{N_{Re}}{3}\ln\left(\frac{P_1}{P_2}\right)\right] \quad (4)$$

The first right-hand term accounts for wall friction and the second for momentum changes due to expansion. If the second term is negligible, the equation reduces to the Poiseuille-Meyer equation. Equation (4) is analogous to one developed by Dodge (2) for isothermal compressible turbulent flow. The numerical coefficients for the momentum term in the two equations differ because of the different velocity profile in viscous and turbulent flow.

By substituting the isothermal sonic velocity squared for RT/M, a differential pressure drop equation is obtained which clearly shows the dependence of the flow on the isothermal Mach number:

$$\frac{dP}{dL} = -\frac{32\mu\overline{U}}{D^2}\Big/\left(1 - \frac{4}{3}\overline{Mai}^2\right) = \left(\frac{dP}{dL}\right)_i\Big/\left(1 - \frac{4}{3}\overline{Mai}^2\right) \quad (5)$$

The term $-32\mu\overline{U}/D^2$ is the pressure gradient for viscous flow in which momentum changes are negligible. The ratio $(dP/dL)/(dP/dL)_i$ is plotted vs. $\overline{Mai}$ in Figure 1. Also plotted in Figure 1 is $(dP/dL)_f/(dP/dL)_i$, where $(dP/$

$dL)_f$ is the pressure gradient due to shear stress at the wall. For Equation (5), $(dP/dL)_f/(dP/dL)_i$ is 1 for all $\overline{Mai}$.

According to Equation (5), dP/dL approaches infinity as $\overline{Mai}$ approaches 0.866, indicating an upper limit for the velocity obtainable in compressible viscous flow in tubes of uniform cross section. As shown later, the velocity profile flattens as $\overline{Mai}$ becomes large, and the upper limit for $\overline{Mai}$ is probably 1.0 rather than 0.866.

VELOCITY PROFILE ANALYSIS

If the velocity profile flattens as $\overline{Mai}$ increases, the velocity gradient at the wall will become steeper, and $(dP/dL)_f$ should increase. Equation (4) was derived on the basis that the mean velocity, mean squared velocity, and wall shear stress could be predicted from the normal parabolic velocity profile. The following analysis takes into account the change in velocity profile.

The axial component Navier-Stokes equation for steady, isothermal, radially symmetric flow in cylindrical coordinates when the radial velocity V and the term $\mu\partial^2U/\partial L^2$ are negligibly small is:

$$\rho U\frac{\partial U}{\partial L} = -\frac{dP}{dL} + \frac{\mu}{r}\frac{\partial}{\partial r}\left[r\frac{\partial U}{\partial r}\right] \qquad (6)$$

and the continuity equation is

$$\frac{d(\rho U)}{dL} = 0 \qquad (7)$$

If it is assumed that P and therefore dP/dL, ρ, and $d\rho/dL$ do not vary with r, it can be shown from continuity and the ideal gas law that

$$\frac{\partial U}{\partial L} = -\frac{UM}{RT}\left(\frac{dP}{dL}\right) \qquad (8)$$

Substituting for $\partial U/\partial L$ in Equation (6) and rearranging, we get

$$\left[1 - \frac{U^2M}{RT}\right]\frac{dP}{dL} = (1 - Mai^2)\frac{dP}{dL} = \frac{\mu}{r}\frac{\partial}{\partial r}\left[r\frac{\partial U}{\partial r}\right] \qquad (9)$$

Although Equation (9) is analytically intractable, numerical solutions for the velocity profile were obtained by machine computation and are presented in Figure 2.

The progressive flattening of the velocity profile with increasing $\overline{Mai}$ can be readily seen. This flattening somewhat invalidates the assumption that the radial velocity is negligible and also somewhat invalidates its consequence that $\rho U(\partial U/\partial L)$ can be replaced by $Mai^2(dP/dL)$.

Neglecting the radial velocity V essentially leads to an unwarranted dropping of the $\rho V(\partial U/\partial r)$ term and miscomputing the $\rho U(\partial U/\partial L)$ term in the Navier-Stokes equation. Analysis of these errors at $\overline{Mai} = 0.44$ indicates that they represent 2.2 and 14.2%, respectively, of $Mai^2(dP/dL)$, the term used to compute the momentum change due to expansion. These errors, while not negligible, should not change the qualitative nature of the curves. Their correction should lead to only slightly less flat velocity profiles and slightly smaller velocity gradients at the wall.

Values for dP/dL and $(dP/dL)_f$ were also obtained in solving Equation (9). The ratio of these values to $(dP/dL)_i$ are plotted in Figure 1 where they can be compared with the corresponding ratios obtained from Equation (5).

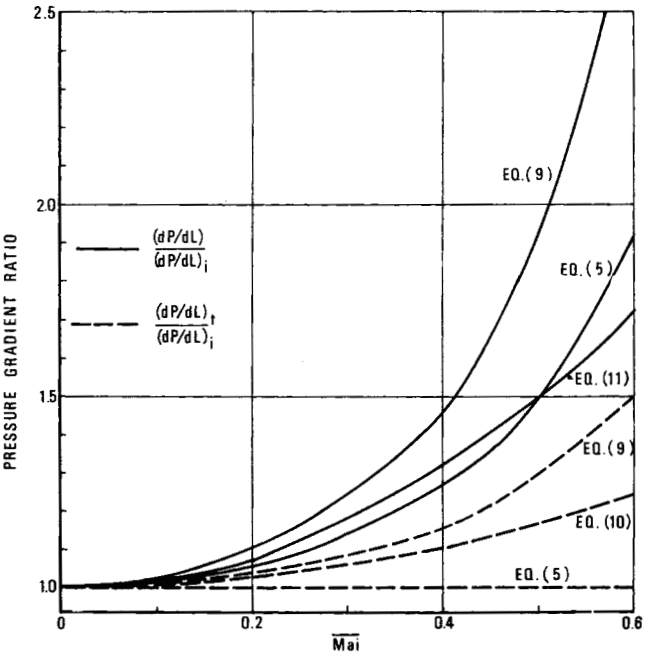

Fig. 1. Pressure gradient ratios vs. $\overline{Mai}$.

The pressure gradients predicted by Equation (9) are significantly higher than those predicted by Equation (5). The incremental pressure gradient for Equation (9) can be seen to be due to the increased wall shear stress brought about by the steeper wall velocity gradients accompanying the flatter profile.

If the corrections for $\rho V(\partial U/\partial r)$ and $\rho U(\partial U/\partial L)$ were put into effect, the $(dP/dL)/(dP/dL)_i$ curve for Equation (9) would fall midway between the present Equation (9) curve and the corresponding curve for Equation (5).

Use of the dP/dL results obtained from Equation (9) requires time-consuming numerical or graphical integration. However, it can be seen that the $(dP/dL)/(dP/dL)_i$ curve for Equation (9) is fairly similar in shape to the curve for Equation (5), and consequently it can be fairly well fitted between $0 < \overline{Mai} < 0.5$ by $1/(1 - 2\overline{Mai}^2)$, a

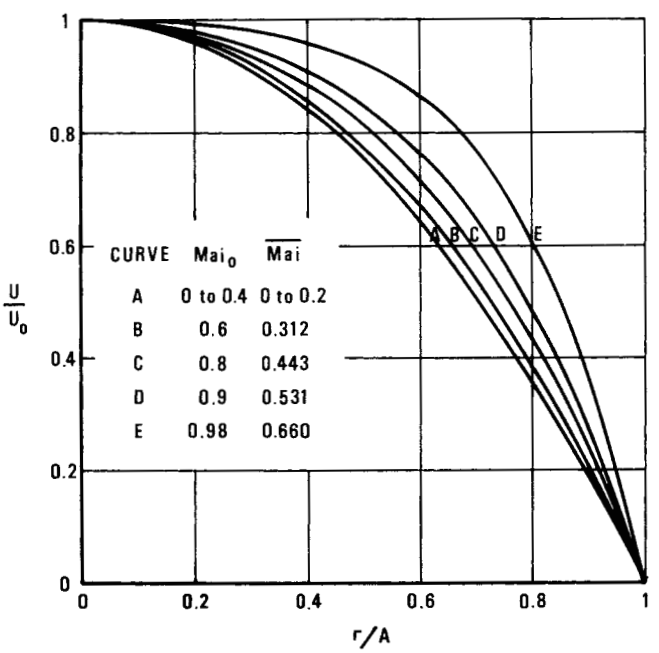

Fig. 2. Velocity profiles at various $\overline{Mai}$ and Mai_0 values.

simple empirical modification of the expression used to generate the curve for Equation (5). If one roughly takes into account the corrections to Equation (9), the corresponding expression would be $1/(1 - 5\overline{Mai}^2/3)$. With the $(dP/dL)/(dP/dL)_i$ expression in this form, it can be readily integrated to yield an equation identical in form to Equation (4) but having [where $\rho V(\partial U/\partial r)$, $\rho U(\partial U/\partial L)$ corrections are applied] a coefficient of 5/12 instead of 1/3 for the N_{Re} ln (P_1/P_2) term.

Kuo's velocity profile equation can be differentiated to obtain $\partial U/\partial r$ at the wall and $(1/r)\partial(r\ \partial u/\partial r)/\partial r$, yielding the following pressure gradient ratio expressions:

$$(dP/dL)_f/(dP/dL)_i = 1 + 2\overline{Mai}^2/3 \qquad (10)$$

$$(dP/dL)/(dP/dL)_i = 1 + 2\overline{Mai}^2 \qquad (11)$$

These are plotted in Figure 1. Equation (11), in contrast to Equation (5) or its empirical corrections, does not indicate the existence of an upper velocity limit. Equation (11), when integrated, yields

$$P_1^2 - P_2^2 = \frac{8\mu RTG}{DM}\left[\frac{8L}{D} + \frac{N_{Re}}{4}\ln\left(\frac{MP_1^2 + 2G^2RT}{MP_2^2 + 2G^2RT}\right)\right] \qquad (12)$$

This equation appears considerably different from Kuo's equation for pressure drop. It is similar in form to Equation (4), but the ln term is considerably more complex. In contrast to Kuo's pressure drop equation, it does reduce to the Poiseuille-Meyer equation at low velocities.

EQUIPMENT AND PROCEDURE

The apparatus used is shown in Figure 3. Steam was generated in an atmospheric pressure boiler and passed through a metering valve into the previously evacuated vacuum system. There, it successively passed through a calming section and the test line across which the flow pressure drop was measured. The steam then entered a large chamber where most of it was condensed as ice as it passed down the front surface and then up the rear surface of a 4.3 sq. ft. panelcoil maintained at −15° to −25°F. A refrigeration system, modified to maintain a noncycling constant Freon evaporation pressure, was used to cool the panelcoil.

Noncondensible gases (that is, air) plus a very slight amount of remaining steam then passed through a line to the vacuum pump. A trap cooled by dry ice-acetone removed almost all the remaining water vapor. The noncondensibles then passed through the pump. After a test, the system was shut down and the condensate allowed to melt. The weight of the collected condensate divided by the steam bleed time (1 hr.) was very nearly equal to the total weight rate of flow.

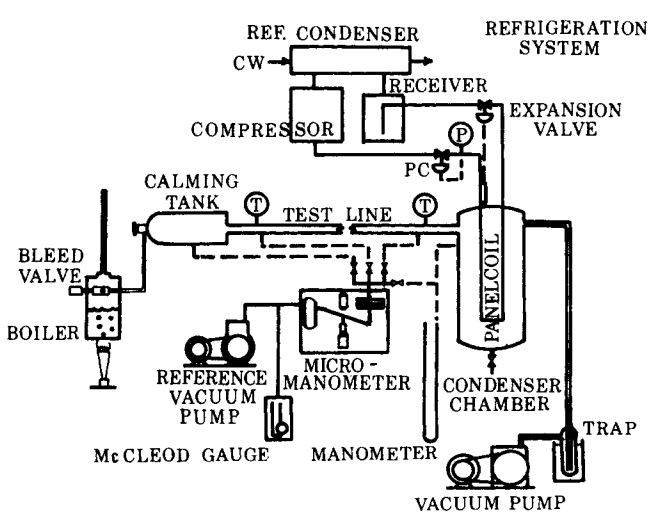

Fig. 3. Apparatus.

During flow, static pressures were measured at taps 548 cm. apart, one 30.5 cm. downstream from the entrance and the other 30.5 cm. upstream from the discharge of the 3.44 cm. I.D. test pipe, and at taps in the calming section and condenser chamber. A micromanometer, readable to 0.0001 in. and with dioctyl sebacate used as the manometric fluid, was used. One leg of the micromanometer was connected through a manifold to the various taps. In most instances the other or reference leg was connected to a separate vacuum space, free of condensible vapor. The absolute pressure in this space was measured by a McCleod gauge. The absolute pressure at a given tap was therefore the differential pressure indicated by the micromanometer plus the reference pressure.

At the highest velocities tested, where the differential pressure could not otherwise be accommodated by the micromanometer, the pipe line and calming tank pressures were measured with reference to the condenser chamber pressure, and the condenser chamber pressure in turn was measured with reference to the auxiliary vacuum space.

To preclude false reading, all micromanometer readings were taken by approaching equilibrium from above and below.

Temperatures were measured along the pipe by three thermometers whose bulbs were attached to the pipe wall and covered with insulation. The ambient temperature was also noted.

In addition to the various steam flow tests, vacuum pump-down tests were carried out to determine the volumetric pumping capacity of the vacuum pump used.

RESULTS

The tabulated pressures, temperatures, and condensate weights for the various run are on file.* In addition to water vapor, a small amount of leakage air passed through the test section. A procedure based on the volumetric pumping capacity of the vacuum pump used for air removal and the pressure drop in the pump line was used to calculate these air flow rates. This procedure, the calculated air flow rates, water vapor flow rates, and total flow rates are also on file.* The leakage air flows were about 1% of the total flow, and possible errors in their calculation can only introduce negligible errors in the total flow rates.

According to Langhaar's criteria (5), the flows tested, with the exception of the lowest velocity runs, were not quite fully developed at the upstream tap of the test section. The small entrance effect corrections for the effective L, which are therefore necessary, were calculated by using Langhaar's method as described in an appendix.*

Values of P_1, P_2, $P_1^2 - P_2^2$, N_{Re}, $\overline{U}_2$, and $\overline{Mai}_2$ are presented in Table 1. Also presented are the right-hand side values for Equation (4), Equation (4) modified by using a 5/12 coefficient for the N_{Re} ln (P_1/P_2) term to empirically allow for the flattening of the velocity profile, and Equation (12). The right-hand side values are based on corrected effective values for L. The percentage difference between these right-hand side values and the corresponding $P_1^2 - P_2^2$ values are also tabulated. $P_1^2 - P_2^2$ is plotted vs. the right-hand side of Equation (4) in Figure 4.

The average deviation for Equation (4) is somewhat less than for the other equations. Furthermore, the deviations for modified Equation (4) and Equation (12) are largest at high velocities, where the equations are subjected to their most critical test.

* Tabular material has been deposited as document 01080 with the ASIS National Auxiliary Publications Service, c/o CCM Information Sciences, Inc., 22 W. 34th St., New York 10001 and may be obtained for $2.00 for microfiche or $5.00 for photocopies.

Table 1. Flow Correlations

Run No.	P_1 (μ Hg)	P_2 (μ Hg)	N_{Re}	$\bar{U}_2$ (ft./sec.)	$\overline{Mai_2}$	Right-hand sides $P_1^2 - P_2^2$	Equation (4) [10^6 (μ Hg)^2]	Modif. Equation (4)	Equation (12)	Percent deviation Equation (4)	Modif. Equation (4)	Equation (12)
1	1,855	941	385	381	0.312	2.556	2.472	2.515	2.530	−3.28	−1.61	−1.02
2	1,785	840	388.5	427	0.352	2.481	2.485	2.525	2.540	+0.16	+1.77	+2.38
3	1,348	815	195.5	222	0.183	1.153	1.179	1.186	1.192	+2.20	+2.80	+3.31
4	1,111	902	70.3	71.5	0.059	0.421	0.411	0.412	0.412	−2.37	−2.25	−2.14
5	2,577	1,500	702	427.5	0.352	4.391	4.560	4.665	4.695	+3.85	+6.24	+6.92
6	2,830	1,410	895	583	0.481	6.021	6.250	6.470	6.430	+3.66	+7.19	+6.55
7	3,315	1,760	1,150	571	0.477	7.892	7.770	8.080	8.010	−1.55	+2.51	+1.50
						Average (absolute)				2.43	3.48	3.41
						Average (with sign)				+0.38	+2.38	+2.50

At high velocities, the predicted and observed $P_1^2 - P_2^2$ values are significantly higher than those predicted by the Poiseuille-Meyer equation. At the highest flow rate tested, for example, Equation (4) predicts a $P_1^2 - P_2^2$ value which is 19% higher than the Poiseuille-Meyer value. For the same mass flow rate and exit pressure, the percentage increase will become greater as the pipe length decreases.

The deviations from Equation (4) are of the order of the ascribable sources of experimental error. Slight drifts in the reference pressure and in the micromanometer zero setting were observed and may account for a 1 to 2% error in pressure measurements.

It is curious that Equation (4) fits the experimental data somewhat better than either of the equations which take profile flattening and increased wall drag into account. In part this may be due to Equation (4), on the basis of a constant parabolic profile, somewhat overaccounting for the momentum changes due to expansion.

Nonisothermal conditions may account for part of the success of Equation (4). For adiabatic flow at the maximum velocity tested, the average temperature of the gas would decrease 6.3°K. due to its increase in kinetic energy. Rough analysis indicates that heat transfer, under the conditions used, would have limited this temperature drop to about 2.9°K. below ambient. Such a temperature drop, when averaged over the test section, would produce a 1% lowering of the right-hand sides of the tested equations, an effect which could not be reliably detected. The temperatures measured at the entrance to the test section, the portion nearest the steam generator, were a few degrees above ambient and 2° to 5°K. higher than the temperatures at the middle and far end of the test line, indicating rapid equilibration of the temperature of the flowing steam and the environment.

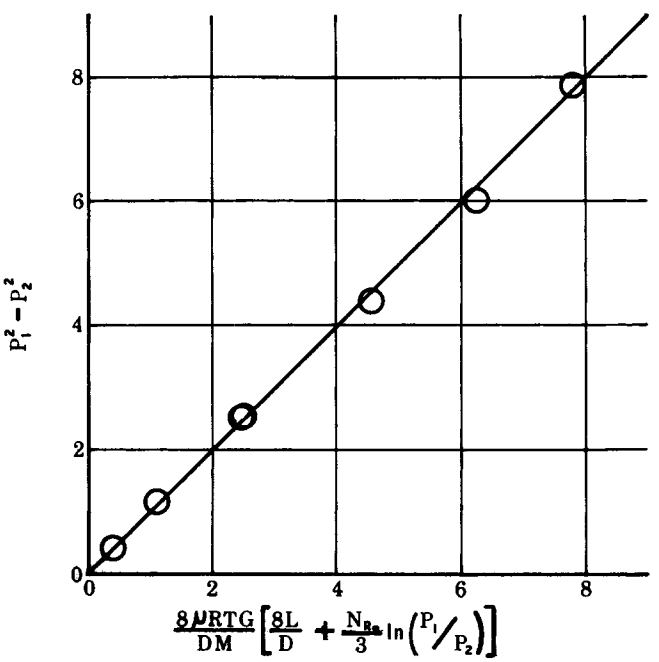

Fig. 4. $P_1^2 - P_2^2$ vs. $\frac{8\mu RTG}{DM}\left[\frac{8L}{D} + \frac{N_{Re}}{3}\ln\left(\frac{P_1}{P_2}\right)\right]$

Units: 10^6 (Microns Hg)^2.

While the adiabatic temperature drop at the maximum velocity tested would average only 6.3°K., if no conduction occurred, the temperature at the axis of the pipe would drop 25°K. This region is least accessible to heat transfer to the outside, and significant gradients in T and μ might therefore exist. If such gradients did exist, they would help preserve a near parabolic profile and favor greater conformity with Equation (4).

The entrance effect correction had an effect of roughly 4% on the pressure drop equations at the highest velocity tested. Because of the flattening profile, the entrance effect correction should be somewhat smaller than for normal parabolic flow. A reduced entrance effect correction would somewhat improve the fit between the experimental data and modified Equation (4) or Equation (12).

Because of the reasons just cited and the smallness of the difference of the computed results, 4% at the highest velocity tested, it is difficult to conclude that Equation (4) is preferable to the equations which account for profile flattening. In order to resolve this question, further tests at higher $\overline{Mai}$ values and in pipes of various sizes are planned. Because of the marked flattening in the velocity profile indicated by Figure 2 at $\overline{Mai}$ greater than 0.5, Equation (4) is not recommended for use above the range for which it has been tested to date.

ACKNOWLEDGMENT

The authors are grateful for a grant from the Maxwell House Division of the General Foods Corporation which made possible the purchase of test equipment used in this study.

NOTATION

A = tube radius
D = tube diameter
$(dP/dL)_f$ = pressure gradient due to friction
$(dP/dL)_i$ = pressure gradient for flow with negligible momentum change due to expansion
G = mass flux, flow per unit area per unit time
L = tube length, axial distance

M = molecular weight
Mai = local isothermal Mach number
$\overline{Mai}$ = average isothermal Mach number for cross section
N_{Re} = Reynolds number
P = pressure
R = perfect gas law constant
r = radial distance
T = absolute temperature
U = local axial velocity
$\overline{U}$ = average axial velocity for cross section
$\overline{U^2}$ = mean square axial velocity for cross section
V = radial velocity
μ = viscosity
ρ = density
τ_w = local wall shear stress
$\bar{\tau}_w$ = average wall shear stress for given length of tube

Subscripts

0 = at center line
1 = upstream tap
2 = downstream tap

LITERATURE CITED

1. Bird, R. B., W. E. Stewart, and E. N. Lightfoot, "Transport Phenomena," p. 211, Wiley, New York (1960).
2. Dodge, B. F., "Chemical Engineering Thermodynamics," p. 350, McGraw Hill, New York (1944).
3. Dushman, S., "Scientific Foundations of Vacuum Technique," 2 ed., p. 82, Wiley, New York (1962).
4. Kuo, Y. H., *J. Math Phys.*, **22**, 13-30 (1943).
5. Langhaar, H. L., *Trans. Am. Soc. Mech. Engrs.*, **64**, A-55 (1942).
6. Shang, J., and M. H. Bloom, *Polytechnic Inst. of Brooklyn Aeronautical Lab. Rept. No. 749* (May 1962); N62-13611 Ad278 128.

Manuscript received October 22, 1968; revision received January 31, 1969; paper accepted February 3, 1969.

A New Technique for Chemical Kinetics at High Pressures

R. A. GRIEGER and C. A. ECKERT

University of Illinois, Urbana, Illinois

Information about the transition state of a chemical reaction is quite useful for the determination of mechanisms and for design of solvents for the reaction. High pressure kinetic studies, if sufficiently accurate, provide the required data. This work reports a new technique developed for measuring rates of chemical reactions in solution at high pressure. This method involves in situ mixing of reactants under pressure and direct sampling for analysis, eliminating large errors of temperature equilibration and time measurement inherent in existing techniques, and thus yielding more accurate results. Experimental results for the Diels-Alder reaction of isoprene and maleic anhydride are reported at pressures up to more than 6,000 atm.

A new technique for high pressure chemical kinetics has been developed for very precise determinations of volumes of activation. By eliminating two sources of significant uncertainty inherent in previous methods, errors in time and temperature, activation volumes may be measured with an accuracy better than 1 cc./g.-mole. The technique proposed here includes the first reported application of in situ initiation of the reaction, avoiding errors in temperature due to the heat of compression or the thermal lag of a heavy steel vessel. Analyses were carried out by continual sampling, at pressures more than twice as high as those at which previous high pressure sampling had been reported (*7, 11*), permitting much more accurate time measurements than would be obtained by the classical method of disassembly of the vessel for analysis.

The effect of pressure on the rate of a chemical reaction yields important information about the structure and properties of the transition state for the reaction. The activated complex theory of Evans and Polyani (*6*) provides a theoretical basis for interpretation of high pressure kinetic data. Using this approach, and expressing the rate constant in pressure invariant concentration units (such as the rate constant in mole fraction k_x), one may show rigorously (*8*) that the measured effect of pressure gives the volume of activation $\Delta V^{\ddagger}$, the difference in partial molal volume between the transition state for the reaction and the reactants:

$$\left(\frac{\partial \ln k_x}{\partial P}\right)_T = -\frac{\Delta V^{\ddagger}}{RT} \qquad (1)$$

The volume of activation represents the second derivative of the actual physical measurement, concentration as a function of time. Thus it is essential that the data taken be as accurate as possible. Frequently, a relatively small difference in activation volume may have significant meaning. For certain reactions, such as the Diels-Alder reaction, a difference in activation volume of approximately

R. A. Grieger is at the University of Wisconsin, Madison, Wisconsin.